Perugia, 13-14 aprile 2023, Università degli Studi di Perugia

XXIII Congresso Nazionale CIRIAF

Sviluppo Sostenibile, Tutela dell'Ambiente e della Salute Umana

Monitoring the thermal potential of low-cost radiative cooling materials under static and dynamic conditions of exposure

Chiara Chiatti [1], Ioannis Kousis [2], Claudia Fabiani [2], Laura Carlosena [3] and Anna Laura Pisello [1,2]*

[1] CIRIAF Research Centre – University of Perugia, Via G. Duranti 67, 06125 Perugia (Italy)

[2] Engineering Department – University of Perugia, Via G. Duranti 93, 06125 Perugia (Italy)

[3] Department of Engineering – Universidad Pública de Navarra, Campus de Arrosadía, 31006 Pamplona, Navarra (Spain)

* Author to whom correspondence should be addressed. E-Mail: anna.pisello@unipg.it

Abstract: Reflecting the radiation of the sun while emitting thermal radiation to cold outer space has proven to be an effective solution against urban overheating. The latter severely impact the energy consumption of buildings, outdoor pollution levels, and heat-related morbidity and mortality, which is why recent research has focused on new advanced mitigation technologies to be implemented in cities. Passive radiative cooling (PRC) has the potential to provide a temperature lower than ambient without any energy consumption. While conventional cooling prototypes reject heat to the air, PRCs reject heat to the outer atmosphere emitting radiation mainly in the 8-13 µm range, i.e., the so-called atmospheric window. This work investigates the thermal behavior of different radiative cooling materials under various exposure conditions to examine their effective cooling potential. The basic structure of the samples comprehends a highly reflective substrate (aluminum or Vikuiti) and a silica-derived emissive layer. After a preliminary characterization under controlled environmental settings, the samples were exposed outdoors, and their superficial temperature was monitored during the central hours of the day. Comparisons among samples and a benchmark aluminum reference layer were made, also considering the weather data collected during the days of exposure. Although the samples did not reach sub-ambient temperatures during the monitoring, the emissive layer significantly reduced the surface temperature. Furthermore, the effect of a tunable intermediate layer placed between the substrate and the emissive element was demonstrated to positively impact

ISBN (online PDF) 978-88-9392-442-9
Published by Morlacchi Editore University Press.

Cod_040_pp_532

the thermal performance of the sample, thanks to its capability of changing the emissivity spectrum with temperature.

Keywords: radiative cooling; urban heat island; spectrally selective materials; cool materials; in-field monitoring.

1. Introduction

Human activity over the last century has contributed significantly to the ongoing climate crisis, leading to an increase in average global temperatures and elevated ambient temperatures in cities worldwide [1]. Materials used in urban areas that absorb and store solar radiation, combined with a lack of greenery and water bodies, contribute to the higher incidence of urban overheating, particularly during hot periods [2],[3]. This leads to a significant increase in energy demand for cooling, resulting in high energy consumption and greenhouse gas emissions. Buildings are particularly responsible for this issue: they account for over 30% of global final energy consumption and nearly 30% of greenhouse gas emissions, and most electricity and heat generating systems rely on fossil fuels [4],[5]. Studies have shown that in urbanized areas, high temperatures can cause discomfort both indoors and outdoors. Unfortunately, extreme heat events are becoming more frequent and can even lead to increased morbidity and mortality rates [6], particularly among vulnerable social groups who may lack access to adequate energy services [7]. As a result, several heat dissipation strategies have been proposed and tested to improve the thermal urban environment for both indoors and outdoors.

Passive cooling techniques have gained significant attention in recent years, and Radiative Cooling (RC) is among the most promising ones. Its main goal is to decrease building surface temperatures and regulate indoor conditions, while also contributing to decreasing urban ambient temperatures. PRC occurs naturally during nighttime when direct sunlight is absent. It works by utilizing a surface that highly emits thermal radiation within the Infrared (IR) wavelength range, particularly within the Atmospheric Window (AW) where the atmosphere is nearly transparent. At these wavelengths, thermal radiation goes directly to outer space without being trapped by Earth's atmosphere. The higher the emission within the AW range, the lower the heat exchange with the atmosphere, resulting in lower surface temperatures [8]. However, during daytime, simply emitting within the AW range is insufficient for reducing surface temperature because heat gains from incident sunlight outweigh the surface's thermal emission. To achieve Daytime Radiative Cooling (DRC), it is therefore essential to simultaneously reflect shortwave radiation through high reflectance. Until recently, the production of materials that can both highly reflect shortwave radiation and highly emit thermal radiation almost exclusively within the AW range was limited due to the absence of sophisticated fabrication technologies. Although nighttime RC has been investigated since the 1970s, it was not until 2014 when Raman et al. [9] successfully developed and experimentally tested a RC structure that achieved sub-ambient temperature during direct exposure to the sun, making it the first-ever material to achieve

ISBN (online PDF) 978-88-9392-442-9 -
Published by Morlacchi Editore University Press.

sub-ambient temperature of up to almost 5 °C in the daytime. This breakthrough triggered relevant research for built environment applications, and DRC is currently considered the next generation of materials for super-cool building skins [8],[10].

The literature describes two main types of DRC, i.e., selective and broadband RC, both with a high capacity of reflecting the incident solar radiation (>90%). Selective radiative cooling (SDRC) materials emit thermal radiation specifically within the AW (8-13 μm) and can achieve significant surface temperature reductions (up to 40 °C under ideal conditions) [9],[11]. SDRCs are ideal for decreasing indoor temperatures and improving building energy efficiency. Broadband DRCs, on the other hand, emit within the overall Infrared spectrum (IR) and inherently exchange power with the atmosphere [12]. BDRCs are effective for sub-ambient surface temperature and urban overheating mitigation by transferring their cooling effect to the ambient.

Studies on DRCs have shown that they can significantly reduce surface temperatures and have strong cooling capabilities, making them a promising option for the next generation of building materials to counteract urban overheating. However, their practical use is limited by high costs and complex manufacturing processes. Moreover, there are no established standards or protocols for monitoring DRCs in the laboratory or in real-world settings, which can lead to biased comparisons of results. Therefore, while DRCs show great potential, there are still significant challenges that need to be overcome for their widespread adoption. In this framework, the present work aims to study low-cost scalable prototypes for daytime radiative cooling as possible materials to be implemented in the built environment. Their thermal behavior is evaluated under different meteorological and boundary conditions, by means of a dedicated experimental methodology involving both in-lab and in-field tests.

2. Materials and Samples

This research focuses on testing different radiative cooling prototypes developed and optimized from a prior study [13]. The basic structure was made of a reflective aluminum substrate and an emissive silica coating, following the same approach proposed by C.G. Granqvist and A. Hjortsberg [14]. In particular, the emissive layer was a spray coating made of PMSQ (polymethylsilsesquioxane) with SiO_2 nanoparticles embedded at a 5% weight. The approximate cost for the proposed emissive layer of 2 μm of PMSQ and SiO_2 nanoparticles is about 0.3 €/m^2, being competitive for built-environment applications [13]. Table 1 and Figure 1 summarize all the considered prototypes.

Samples AS-1 and AS-2 belong to the basic class of materials; the only difference is that AS-2 was fabricated with an enhanced formulation to improve both the solar transparency of the emissive layer and the reflectivity of the substrate. In VS sample, instead, the aluminum layer was substituted with a 3M Vikuiti Enhanced Solar Reflector (ESR) film [15] to optimized the reflectivity of the substrate. Finally, AWS sample was made of the aluminum substrate, the improved emissive layer based on PMSQ and SiO_2 and a tunable layer with developed vanadium dioxide doped with tungsten, placed between the two. A traditional aluminum sheet (sample A) was also investigated and taken as reference to evaluate the performance of the multi-layered structure of the radiative cooling prototypes.

ISBN (online PDF) 978-88-9392-442-9 -
Published by Morlacchi Editore University Press.

Table 1. Summary of the considered samples.

Sample code	Substrate	Tunable layer	Emissive layer	Thickness [mm]	Dimensions [mm×mm]
A	aluminum	-	-	0.05	110×110
AS-1	aluminum	-	PMSQ + SiO_2 nanoparticles	1.00	50×50
AS-2	aluminum	-	PMSQ + SiO_2 nanoparticles	1.00	195×195
VS	vikuiti ESR	-	PMSQ + SiO_2 nanoparticles	0.03	115×115
AWS	aluminum	Tungsten-doped VO_2	PMSQ + SiO_2 nanoparticles	1.00	195×195

Figure 1. Schematic structure (above) and photos (below) of the considered samples.

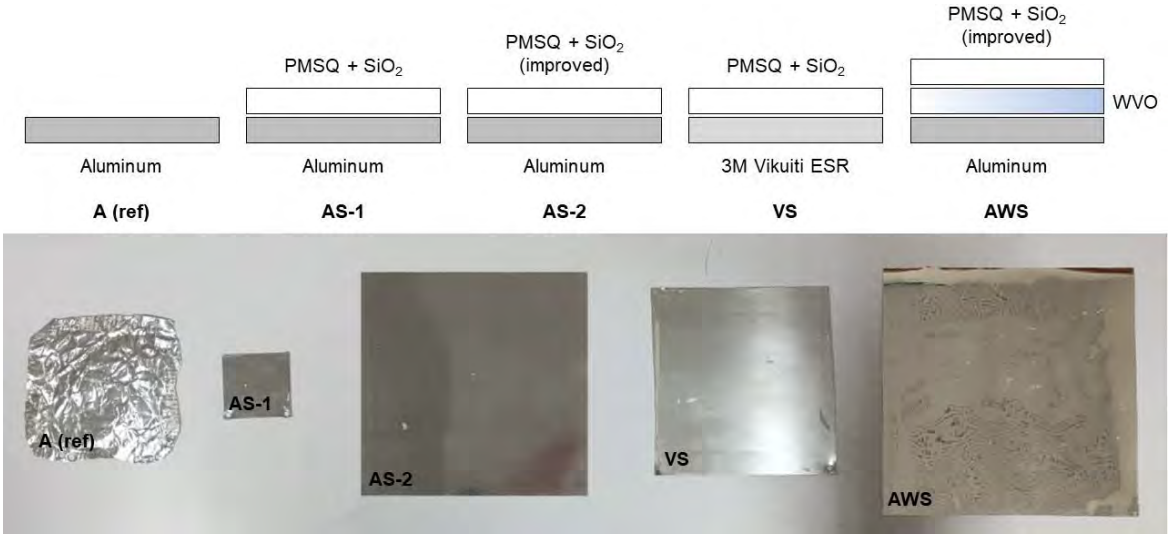

3. Methodology

The aim of this research was to explore the impact of spectral emissivity profile on the potential to achieve sub-ambient temperatures, which can help mitigate urban overheating. To accomplish this objective, the thermal behavior of the selected materials was monitored when exposed to several controlled and realistic outdoor boundary conditions. The performance of PRC materials was compared to the aluminum foil without the emissive layer (sample A). The surface temperature of the samples was continuously measured by three sensors (thermocouples, type T) applied on the downward face of each prototype. Data were collected with a time-step of 10 s and the average value of the three sensors was considered.

3.1. In-lab thermal monitoring

To preliminary evaluate the impact of different relative humidity (RH) and solar irradiation (SR) values, a climatic chamber (ATT DM340SR) equipped with a solar simulator (BF SUN 1200W) was used. Each sample and the reference one (A) were placed together inside the internal compartment of the

ISBN (online PDF) 978-88-9392-442-9 - © 2023 Morlacchi Editore University Press, CC BY 4.0 International.
Published by Morlacchi Editore University Press.

chamber and exposed to a hygrothermally controlled cycle. The cycle covered three levels of solar irradiation (600, 750, 900 W/m2) and two levels of relative humidity (50% and 90%), while keeping a constant ambient temperature of 21°C. An extruded polystyrene base was used to locate the samples to avoid heat conduction. Figure 2 shows the settings of the 30-min scenarios the samples were exposed to.

Figure 2. (a) Temperature (T), relative humidity (RH) and solar irradiation (SR) settings of the six consecutive scenarios the samples were exposed to. (b) DRC and reference sample inside the climatic chamber.

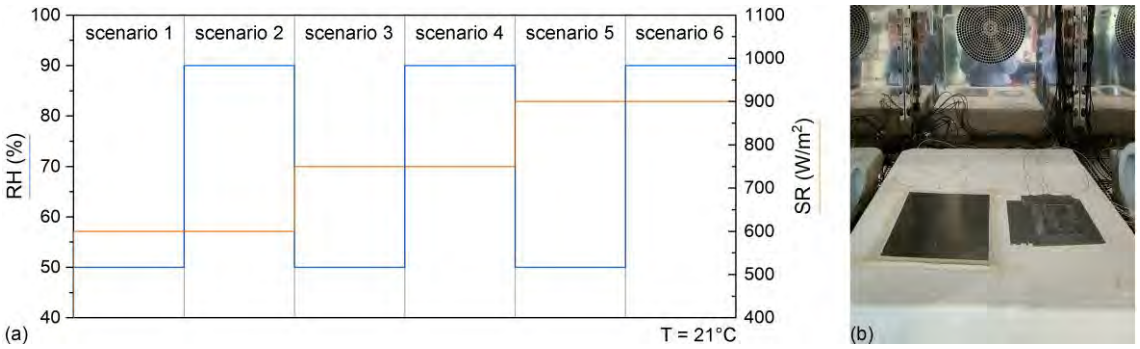

3.2. In-field thermal monitoring

At a later stage, DRC prototypes were directly exposed to the sun on the parking area of the CIRIAF Research Centre (Perugia, Italy). The experiment was repeated for four sunny days, between January 30 and March 17 of 2023, from 12:00 to 16:00. Four experimental setups were investigated, as summarized in Figure 3:

- Samples on a 10-cm thick polystyrene base (scenario O1);
- Samples on a 10-cm thick polystyrene base, placed over a heating plate at 60°C (scenario O2);
- Samples on an aluminum layer, placed over a heating plate at 60°C (scenario O3);
- Samples on an aluminum layer, placed over a heating plate at 90°C (scenario O4).

At the same time, an outdoor monitoring system placed on the rooftop of CIRIAF's building was used to capture the overall microclimatic background boundary conditions.

The system includes a weather station measuring air temperature, wind speed and direction, relative humidity, and incoming solar radiation.

All the sensors perform a continuous monitoring campaign, collecting data every 10 s and producing average values every 10 min. Data are gathered via a connected Data Logger station which is coupled with a web-based platform wherein the sensors' data become available for download.

ISBN (online PDF) 978-88-9392-442-9 - © 2023 Morlacchi Editore University Press, CC BY 4.0 International.
Published by Morlacchi Editore University Press.

Figure 3. Schematic representation of the four experimental setups for outdoor thermal monitoring (above) and picture of their outdoor thermal monitoring under direct sun (below).

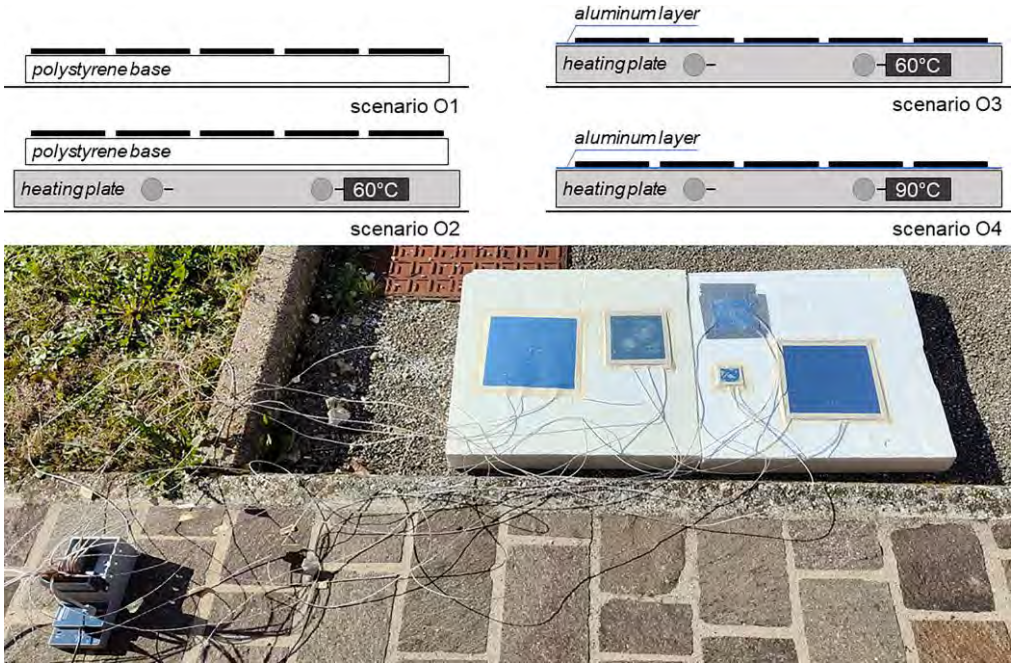

4. Results and discussions

4.1. Results from the in-lab thermal monitoring

Figure 4 shows the superficial temperature profiles of all the DRC samples with respect to the reference aluminum foil during the in-lab monitoring campaign. It is important to note that the samples were not exposed to the real atmosphere, but only to the irradiation provided by the solar simulator of the climatic chamber. As a result, radiative exchange with the sky did not occur, allowing for the evaluation of the impact of different relative humidity (RH) and solar irradiation (SR) intensities on the thermal performance of the samples.

It is evident how the exposure to a higher level of irradiation caused an increase in the samples' superficial temperature, which stayed always above the constant ambient 21°C set inside the climatic chamber. While sample AWS had a close temperature to the aluminum reference, which ranged from ≈30°C (beginning of scenario 1) to ≈38°C (end of scenario 6), all the others PRCs stayed cooler. Starting at 26.7°C, AS1 and AS2 had a superficial temperature increase of 7.8°C and 7.4°C respectively, while VS sample heated by only 6.1°C, resulting in the best performing prototype. Slight changes in temperature, in the range 0.2-0.7°C, can be seen also between those scenarios that differed only for RH values (1-2, 3-4, and 5-6). Despite there are evidence of the worsening of the PRCs performance with high relative humidity [16],[17], we can only hypothesize that something similar happened, because the same increase belonged also to the reference sample A that does not have the emissive layer.

ISBN (online PDF) 978-88-9392-442-9 - © 2023 Morlacchi Editore University Press, CC BY 4.0 International.
Published by Morlacchi Editore University Press.

Figure 4. Superficial temperature's profiles of each DRC sample (continuous line), compared to the reference aluminum foil (dashed line). Thermal monitoring performed inside the internal compartment of the climatic chamber at different RH and SR values (T_{amb} at 21°C).

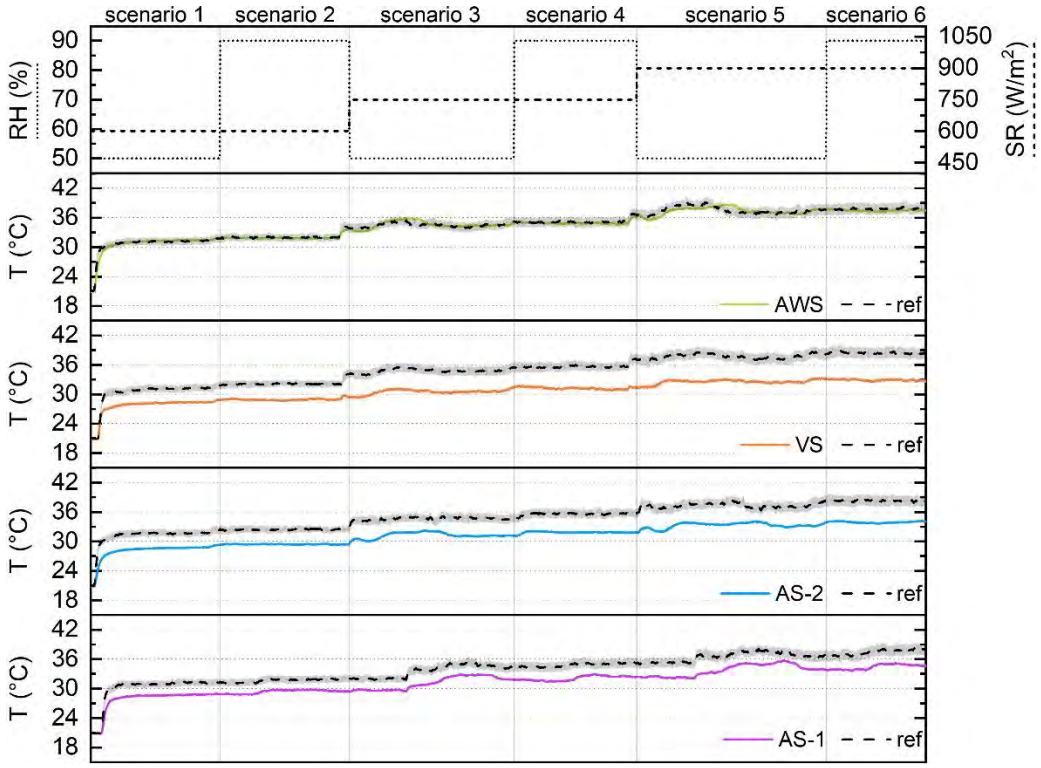

4.2. Results from the in-field thermal monitoring

Figures 5-8 report the results from the monitoring of the thermal behavior of the DRC samples under realistic conditions of exposure. The upper part of the graphs shows the averaged outdoor environmental parameters collected by the microclimatic weather station located on the roof of CIRIAF's building, i.e., solar radiation (SR), air temperature (T_{amb}) and relative humidity (RH). The lowest part of the figures, instead, compares the superficial temperature of each prototype with the reference one (sample A). As introduced in Section 3.2, the same procedure was repeated for different sunny days and according to four different experimental setups (scenarios O1-O4) to evaluate the impact of different boundary conditions on the thermal performance of the PRC prototypes. Table 2 summarizes for each scenario the maximum and minimum values of both (i) surface temperatures and (ii) difference between the reference aluminum and RC material surface temperatures.

By simply exposing all the samples to the sun, placing them on a 10-cm thick polystyrene base to avoid heat conduction (scenario O1, Figure 5), similar relations to what observed during the in-lab campaign occurred. AWS sample reached a superficial temperature very close to, but slightly below (from -0.8°C to -3.3°C), the reference. More significant differences were detected between the other PRCs prototypes and the reference (sample A). As during the in-lab monitoring, the Vikuiti sample (VS) proved to guarantee the highest cooling potential, maintaining the lowest surface temperatures during the whole monitoring with a maximum reduction of 15.8°C with respect to aluminum. Small differences

ISBN (online PDF) 978-88-9392-442-9 - © 2023 Morlacchi Editore University Press, CC BY 4.0 International.
Published by Morlacchi Editore University Press.

can be found, instead, between the behavior of samples AS1 and AS2: the second stayed slightly warmer, with a difference from the former in terms of T_{max} and T_{min} of 1.8°C and 0.7°C, respectively. Given the low air temperatures the materials were exposed to, it was not possible to reach sub-ambient T values: superficial temperatures basically increased and decreased according to the solar irradiation profile, getting close to T_{amb} once SR values went down (from 15:00 to 16:00).

Figure 5. Scenario O1: superficial temperature's profiles of each DRC sample (continuous line), compared to the reference aluminum foil (dashed line). Thermal monitoring performed on 30 January 2023.

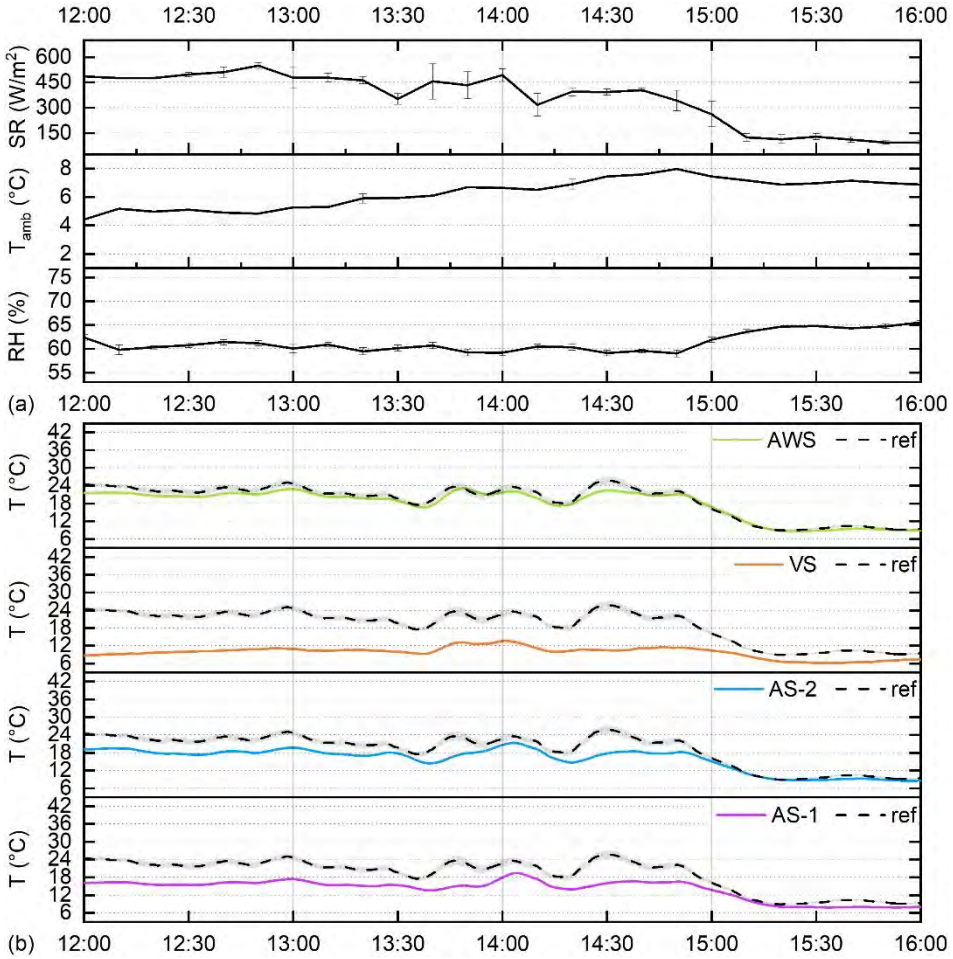

Observation of the thermal behavior of the samples according to scenario O2 (Figure 6) confirmed the best cooling performance of the sample VS with respect to the reference aluminum foil and compared to the other RCs. Of course, placing the polystyrene support on a heating plate at 60°C, made the samples reach higher temperatures than in scenario O1. In particular, the sample RC with the tunable layer between the substrate and the emissive part (sample AWS) exceeded the reference temperature (sample A) throughout the whole monitoring period, up to a maximum difference of 7.1°C in the time-range 14:30-15:00. All the other RCs remained cooler than the aluminum foil, with AS1 behaving slightly better than AS2, and VS performing best (ΔT_{max} = 13.2°C).

ISBN (online PDF) 978-88-9392-442-9 - © 2023 Morlacchi Editore University Press, CC BY 4.0 International.
Published by Morlacchi Editore University Press.

Figure 6. Scenario O2: superficial temperature's profiles of each DRC sample (continuous line), compared to the reference aluminum foil (dashed line). Thermal monitoring performed on 2 February 2023.

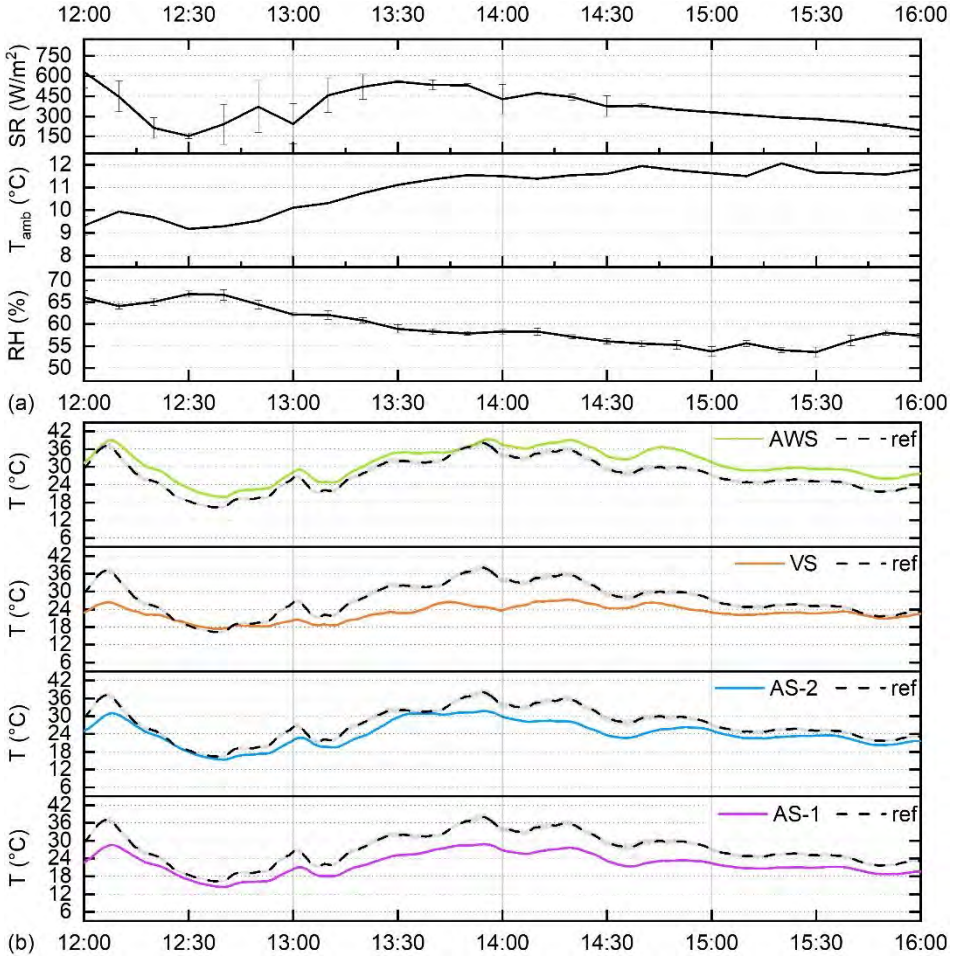

Given the low thermal conductivity of the polystyrene support used in scenario O2, samples did not reach the set temperature of the heating plate (60°C) during the monitoring, making it difficult to assess any radiative cooling phenomenon that may have occurred. For this reason, in scenarios O3 and O4, the samples were placed in direct contact with the heating plate with only a layer of aluminum between them. To be consistent with the last scenario described, the temperature of the heating plate was also set to 60°C in O3; results are shown in Figure 7.

Always comparing the RC materials with the reference A, it is evident how something in the behavior of the former changed at higher temperatures. While the aluminum foil reached an average temperature of 100°C, with oscillations that followed the solar irradiation profile, all the RCs samples stayed cooler. In this case, VS performed worse than the others, reaching an 18.1°C maximum difference from A temperature. AS1, AS2 and AWS, not only maintained their superficial temperature in the range 59.1-68.0°C, i.e., very close to the heating plate temperature, but their profile was almost constant throughout the monitoring, ranging between less than 10°C. Probably, the heating rate of the plate overcame the effect of solar irradiation on the superficial temperature of the samples. Again, AS1

ISBN (online PDF) 978-88-9392-442-9 - © 2023 Morlacchi Editore University Press, CC BY 4.0 International.
Published by Morlacchi Editore University Press.

stayed a bit cooler than the optimized counterpart (AS2), with differences between their T in the range 4.5-6.0°C.

Focusing on the performance of sample AWS, a big change in scenario O3 with respect to O1 and O2, can be noticed. While the RC prototype used to behave very similarly to the aluminum reference, in Figure 7 it showed a superficial temperature reduction with respect to sample A going from 14.2°C up to 43.9°C. This could be related to the activation of the tunable layer, i.e., to changes in the emittance property and radiative power of the overall system, above a certain T value. Indeed, the tunable layer's composition involved vanadium dioxide doped with tungsten: VO_2 has an acknowledged phase transition temperature of 68°C which can be effectively decreased by W-doping [18],[19].

Figure 7. Scenario O3: superficial temperature's profiles of each DRC sample (continuous line), compared to the reference aluminum foil (dashed line). Thermal monitoring performed on 7 February 2023.

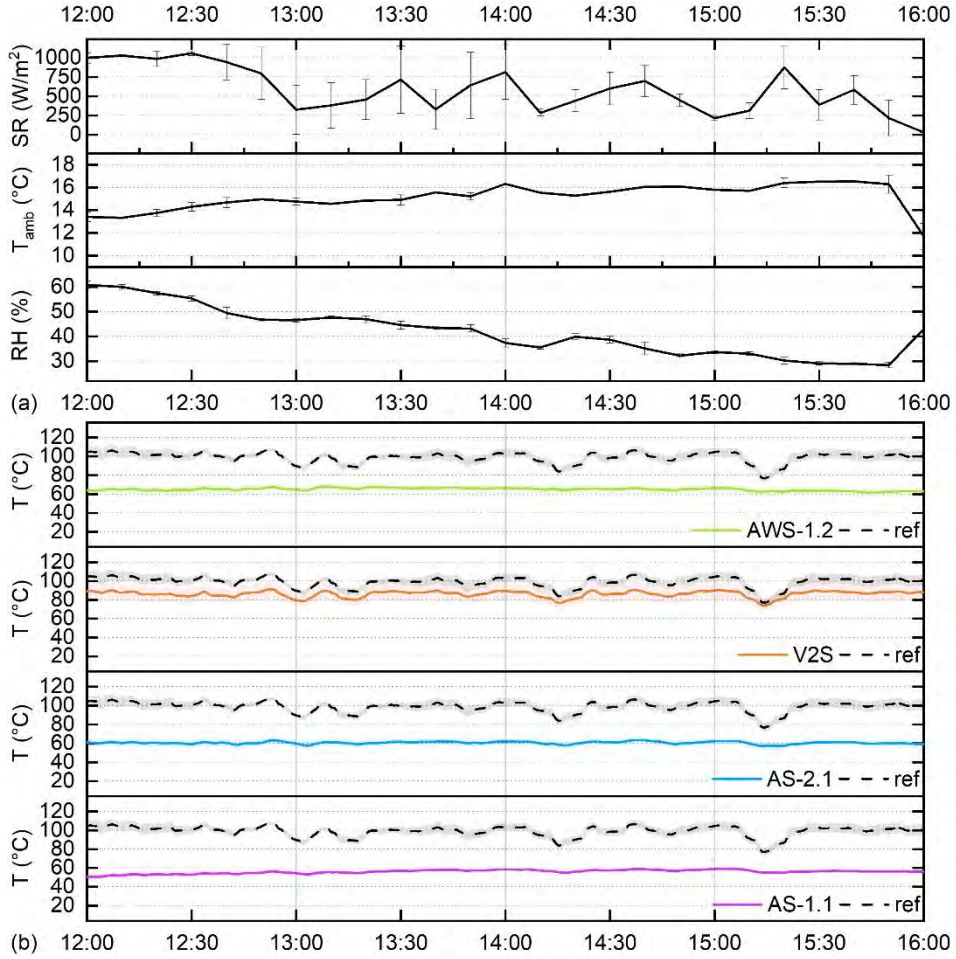

To further investigate the radiative cooling potential of the samples in more extreme boundary conditions, an O3-similar experimental setup was reproduced for scenario O4, setting the temperature of the heating plate at 90°C (Figure 8). While Vikuity sample managed to stay 3.4°C to 15.2°C below the aluminum reference, all the other RC options not only differed more from sample A, but also

ISBN (online PDF) 978-88-9392-442-9 - © 2023 Morlacchi Editore University Press, CC BY 4.0 International.
Published by Morlacchi Editore University Press.

maintained a superficial temperature lower than 90°C, i.e., the temperature of the heating plate. In more details, samples AS1, AS2 and AWS reached a maximum T of 68.7°C, 78.9°C and 78.6°C, respectively. Also in this case, the temperature profile of the RC samples was almost centered to a constant value during the whole monitoring period.

Figure 8. Scenario O4: superficial temperature's profiles of each DRC sample (continuous line), compared to the reference aluminum foil (dashed line). Thermal monitoring performed on 17 March 2023.

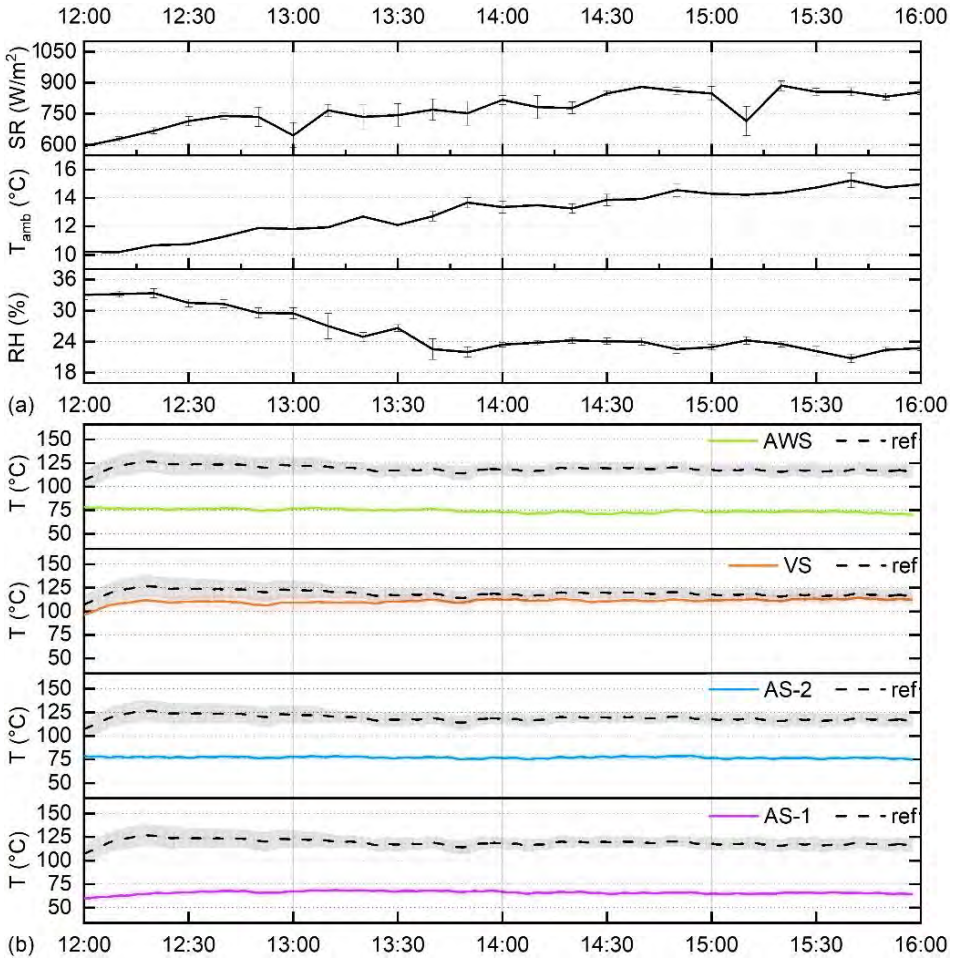

When analyzing the obtained temperature data of each scenario, observations on the geometry of the samples should be considered. As summarized in Table 1, the investigated prototypes differed for dimensions and thickness, and this certainly had an impact on their thermal behavior. For instance, the lower thickness of A and VS with respect to the others helped them reach more easily higher temperatures when placed over a heating source. Despite this, the result of having lower surface temperatures than the one of the heating plate at direct contact with the samples themselves could be of interest thinking of the possible application of such materials as radiative coolers for the built environment. Their capability of maintaining sub-ambient temperatures, even though under extreme boundary conditions, paves the way to further investigation to better detect their radiative cooling potential.

ISBN (online PDF) 978-88-9392-442-9 - © 2023 Morlacchi Editore University Press, CC BY 4.0 International.
Published by Morlacchi Editore University Press.

Table 2. Summary of the measured surface temperatures during the in-field monitoring campaigns.

		A	AS1	AS2	VS	AWS		A	AS1	AS2	VS	AWS
T_{max} (°C)	**Scenario O1**	25.7	19.5	21.3	13.7	23.1	**Scenario O2**	38.0	28.8	31.7	27.2	39.3
T_{min} (°C)		8.9	7.8	8.5	6.2	8.6		16.3	14.4	15.4	17.4	19.8
$\Delta T_{max} = max(T_{ref} - T_{RC})$		-	9.7	8.1	15.8	3.3		-	9.2	7.6	13.2	0.1
$\Delta T_{min} = min(T_{ref} - T_{RC})$		-	0.7	0.03	1.9	0.8		-	1.4	0.1	-1.2	-7.1
T_{max} (°C)	**Scenario O3**	107.2	59.1	63.6	91.1	68.0	**Scenario O4**	126.7	68.7	78.9	114.4	78.6
T_{min} (°C)		76.9	49.9	55.9	74.0	57.2		107.2	60.2	74.9	96.1	70.3
$\Delta T_{max} = max(T_{ref} - T_{RC})$		-	54.4	45.5	18.1	43.9		-	62.1	49.3	15.2	50.2
$\Delta T_{min} = min(T_{ref} - T_{RC})$		-	21.6	19.5	2.8	14.2		-	46.9	28.2	3.4	28.5

5. Conclusions

This study delves into the thermal performance of scalable daytime radiative cooling (DRC) materials. The research examines the evolution of superficial temperature evolution, under different controlled and realistic boundary conditions and in comparison to a simple aluminum foil taken as reference material. The effect of single weather variables, i.e., solar radiation and relative humidity, was first evaluated by exposing the samples to a hygrothermally controlled cycle by means of a climatic chamber equipped with a solar simulator. Excluding the radiative exchange with the sky, it was evident how superficial temperatures increased with the solar irradiation level the samples were exposed to. The prototype with the Vikuiti reflective layer (VS) proved to maintain the lowest temperature in comparison to the reference, followed by AS1 and AS2. The sample with the tunable layer (AWS), instead, behave similarly to aluminum throughout the whole in-lab test.

At a later stage, samples were exposed outdoor to realistic boundary conditions and under direct sun. Four experimental setups (O1-O4) were created during different days (from 12:00 to 16:00), using a heating plate to achieve higher superficial temperatures. Results showed how under most boundary conditions, the RC materials had the ability to stay cooler than the reference aluminum. While VS and AWS were respectively the best- and the worst-performing prototypes at mid-low temperatures (scenarios O1 and O2), their behavior completely reversed for high T values (scenarios O3 and O4). The significant increase in superficial temperature of the Vikuiti sample can be blamed on its small thickness, while the achievement of the transition temperature of the tungsten doped VO_2 activated the tunable layer of the AWS sample, changing its emissive properties.

Future work should investigate the radiative cooling potential of these prototypes more deeply, purifying the results of the possible effects of the different samples' geometry. Their in-lab characterization through optical and thermal techniques of measurement should be performed to assess the absolute properties of each RC prototype. Moreover, the same methodology for outdoor monitoring should be carried out during summer months to detect the possible achievement of sub-ambient temperatures more easily. Finally, the degradation and aging of such materials should be evaluated according to prolonged exposure to realistic and extreme weather conditions.

ISBN (online PDF) 978-88-9392-442-9 -
Published by Morlacchi Editore University Press.

References

[1] Peters GP, Andrew RM, Boden T, Canadell JG, Ciais P, Le Quéré C, et al. "The challenge to keep global warming below 2 °C". Nat Clim Chang [Internet]. 3(1)(2013): 4–6. Available from: http://www.nature.com/articles/nclimate1783

[2] Santamouris M, Cartalis C, Synnefa A, Kolokotsa D. "On the impact of urban heat island and global warming on the power demand and electricity consumption of buildings—A review". Energy Build. 98(2015): 119–24.

[3] Ward K, Lauf S, Kleinschmit B, Endlicher W. "Heat waves and urban heat islands in Europe: A review of relevant drivers". Sci Total Environ [Internet]. 569–570(2016): 527–39. Available from: https://linkinghub.elsevier.com/retrieve/pii/S0048969716312931

[4] Yu X, Chan J, Chen C. "Review of radiative cooling materials: Performance evaluation and design approaches". Nano Energy [Internet]. 88(2021): 106259. Available from: https://linkinghub.elsevier.com/retrieve/pii/S2211285521005152

[5] Kalair A, Abas N, Saleem MS, Kalair AR, Khan N. "Role of energy storage systems in energy transition from fossil fuels to renewables". Energy Storage [Internet]. 3(1)(2021). Available from: https://onlinelibrary.wiley.com/doi/10.1002/est2.135

[6] Khan HS, Santamouris M, Paolini R, Caccetta P, Kassomenos P. "Analyzing the local and climatic conditions affecting the urban overheating magnitude during the Heatwaves (HWs) in a coastal city: A case study of the greater Sydney region". Sci Total Environ [Internet]. 755(2021): 142515. Available from: https://linkinghub.elsevier.com/retrieve/pii/S0048969720360447

[7] Kousis I, Laskari M, Ntouros V, Assimakopoulos M-N, Romanowicz J. "An analysis of the determining factors of fuel poverty among students living in the private-rented sector in Europe and its impact on their well-being". Energy Sources, Part B Econ Planning, Policy [Internet]. 15(2)(2020): 113–35. Available from: https://www.tandfonline.com/doi/full/10.1080/15567249.2020.1773579

[8] Zhao B, Hu M, Ao X, Chen N, Pei G. "Radiative cooling: A review of fundamentals, materials, applications, and prospects". Appl Energy [Internet]. 236(2019): 489–513. Available from: https://linkinghub.elsevier.com/retrieve/pii/S0306261918318373

[9] Raman AP, Anoma MA, Zhu L, Rephaeli E, Fan S. "Passive radiative cooling below ambient air temperature under direct sunlight". Nature [Internet]. 515(7528)(2014): 540–4. Available from: http://www.nature.com/articles/nature13883

[10] Santamouris M, Feng J. "Recent Progress in Daytime Radiative Cooling: Is It the Air Conditioner of the Future?". Buildings [Internet]. 8(12)(2018): 168. Available from: http://www.mdpi.com/2075-5309/8/12/168

[11] Zhou L, Song H, Liang J, Singer M, Zhou M, Stegenburgs E, et al. "A polydimethylsiloxane-coated metal structure for all-day radiative cooling". Nat Sustain [Internet]. 2(8)(2019): 718–24. Available from: https://www.nature.com/articles/s41893-019-0348-5

[12] Kou J, Jurado Z, Chen Z, Fan S, Minnich AJ. "Daytime Radiative Cooling Using Near-Black Infrared Emitters". ACS Photonics [Internet]. 4(3)(2017): 626–30. Available from:

ISBN (online PDF) 978-88-9392-442-9 - © 2023 Morlacchi Editore University Press, CC BY 4.0 International.
Published by Morlacchi Editore University Press.

https://pubs.acs.org/doi/10.1021/acsphotonics.6b00991

[13] Carlosena L, Andueza Á, Torres L, Irulegi O, Hernández-Minguillón RJ, Sevilla J, et al. "Experimental development and testing of low-cost scalable radiative cooling materials for building applications". Sol Energy Mater Sol Cells [Internet]. 230(2021): 111209. Available from: https://linkinghub.elsevier.com/retrieve/pii/S0927024821002518

[14] Granqvist CG, Hjortsberg A. "Radiative cooling to low temperatures: General considerations and application to selectively emitting SiO films". J Appl Phys [Internet]. 52(6)(1981): 4205–20. Available from: http://aip.scitation.org/doi/10.1063/1.329270

[15] "3M™ Vikuiti™ Enhanced Specular Reflector (ESR)" [Internet]. Available from: https://www.3mcanada.ca/3M/en_CA/p/d/v000100093/

[16] Huang J, Lin C, Li Y, Huang B. "Effects of humidity, aerosol, and cloud on subambient radiative cooling". Int J Heat Mass Transf [Internet]. 186(2022): 122438. Available from: https://linkinghub.elsevier.com/retrieve/pii/S0017931021015362

[17] Han D, Ng BF, Wan MP. "Preliminary study of passive radiative cooling under Singapore's tropical climate". Sol Energy Mater Sol Cells [Internet]. 206(2020): 110270. Available from: https://linkinghub.elsevier.com/retrieve/pii/S0927024819305999

[18] Shin E, Pan K, Wang W, Subramanyam G, Vasilyev V, Leedy K, et al. "Tungsten-doped vanadium dioxide thin film based tunable antenna". Mater Res Bull [Internet]. 101(2018): 287–90. Available from: https://linkinghub.elsevier.com/retrieve/pii/S002554081730154X

[19] Taylor S, Yang Y, Wang L. "Vanadium dioxide based Fabry-Perot emitter for dynamic radiative cooling applications". J Quant Spectrosc Radiat Transf [Internet]. 197(2017): 76–83. Available from: https://linkinghub.elsevier.com/retrieve/pii/S002240731630574X

ISBN (online PDF) 978-88-9392-442-9 - © 2023 Morlacchi Editore University Press, CC BY 4.0 International.
Published by Morlacchi Editore University Press.